JOURNAL OF OPTOELECTRONICS AND ADVANCED MATERIALS Vol. 10, No. 11, November 2008, p. 3305 - 3310

About the electromagnetic properties of the Fe-Si-B-Nb-Cu soft magnetic composites

D. IONESCU[a*], I. B. CIOBANU[b]
[a]*Gh. Asachi Technical University of Iaşi, Faculty of Electronics and Telecommunications, 11 Carol I Blvd., 700506 Iaşi, Romania*
[b]*Gh. Asachi Technical University of Iaşi, Department of Physics, 67 D. Mangeron Blvd., 700050 Iaşi, Romania,*

A class of soft magnetic composites has been analyzed in this paper: the Fe-Si-B-Nb-Cu (Finemet) alloys. Materials present a crystalline nanogranular structure, with a unique combination of soft magnetic properties including high permeability and high electrical resistivity. The obtained magnetic properties depend strongly on the microstructure and the phase composition of the primary nanocrystalline phase. We have used the method of structural modeling and simulations for the material characterization in HF fields (1 - 10 GHz in microwave range), considering the effects induced by the nanocrystalline structure. Alloys are multi-phases structures at the atomic scale, presenting magnetic anisotropy. Simulation results were validated by measurements of the constitutive parameters. The magnetic permeability and electric permittivity and conductivity have been calculated on the basis of a physical algorithm for the samples exposed inside a rectangular waveguide. The structural explanation of their evolutions has been pointed out.

(Received January 16, 2008; after revision November 1, 2008; accepted November 27, 2008)

Keywords: Soft magnetic composite, Finemet alloys, Nanocrystalline phase, Structural modeling, Magnetic anisotropy, Microwave range.

1. Introduction

A class of soft magnetic composite (SMC) materials for soft magnetic applications has been considered in this paper: the Fe-Si-B-Nb-Cu (Finemet) alloys. Different compositions for the Finemet alloys have been analyzed in order to determine the elements concentration influence on material properties: $Fe_{74.5}Si_{13.5}B_9Nb_3$, $Fe_{76.5}Si_{13.5}B_9Cu_1$, $Fe_{73.1}Si_{15.5}B_{7.4}Nb_3Cu_1$, $Fe_{73.5}Si_{13.5}B_9Nb_3Cu_1$, $Fe_{74.5}Si_{13.5}B_8Nb_3Cu_1$, $Fe_{77.5}Si_{13.5}Nb_3Cu_1$, as so as the particular structures FIN-1, FIN-2 and FIN-3 ($Fe_{77.5}Si_{11.2}B_{7.2}Nb_{3.3}Cu_{0.8}$, $Fe_{73.2}Si_{13.7}B_{9.5}Nb_{2.7}Cu_{0.9}$ and $Fe_{68.8}Si_{18.6}B_{9.5}Nb_{2.6}Cu_{0.5}$, respectively). The FINs alloy posses a unique combination of soft magnetic properties including high saturation, very low coercivity, high permeability and high electrical resistivity (Yoshizawa *et al*, 1988). Materials are prepared usually by mechanical alloying and the crystallization of the amorphous precursors through an optimum annealing treatment occurs [1]. The obtained magnetic properties depend strongly on the microstructure and the phase composition of the primary nanocrystalline phase (He *et al*, 1994; Tomic, Davidovic, 1996; Coelho, Gomes, de Lima, 2005; Majumdar, Akhtar, 2005; Mudry *et al*, 2007).

In this paper the analysis method of structural modeling and simulations have been used for the material characterization in HF fields (1 - 10 GHz in microwave range), considering of the effects induced by the nanocrystalline structure. Theoretical systems of spins consisting of ferromagnetic nanocrystalline grains immersed in weakly ferromagnetic environment was considered. The interface phenomena, the influence of the grain boundaries, the exchange interactions have to be taken into account. Materials are characterized also by local atomic ordering, with the corresponding interatomic bonding [1], [4], [8]. We have a multi-phases structure at the atomic scale, presenting magnetic anisotropy.

The results obtained by simulation were verified by measurements in the same frequency range.

2. Structure simulation and experimental setup

Our study was performed in order to determine the constitutive parameters (magnetic permeability, electric permittivity and conductivity) of the considered SMC materials and to identify the phase evolving peaks for these parameters. These parameters evolution with frequency was obtained, corresponding to the microwave range.

Determinations are based on simulation of the structure exposed to a variable HF electromagnetic field, with help of a 3D Full-wave Electromagnetic Field Simulation Program (the High Frequency Structure Simulator, HFSS).

Material samples were re-constructed at microscopic level by reproducing the structural configuration of the alloy. The structure details were taken from literature. The previous crystallization studies (Koster, Meinhardt, 1994; Hono, Ping, 1999) indicate that the primary phase changes from the body-centred cubic α-Fe(Si) to the face-centered cubic Fe_3Si (DO_3) on increasing the Si content, or is already the DO_3 (the nanocrystallization can be controlled by modifying the composition) [2]. The Fe_3Si phase induces lower coercivity of the alloys. The Cu atoms role is to form a high density of clusters which become heterogeneous nucleation sites for crystallization. The density of the Cu clusters is of ca. 10^{24} m^{-3}, corresponding to nanocrystals with a grain size of 5 - 20 nm, depending

of the chemical formula [6]. Grain size increases at higher temperatures (above $T_c' \approx 600 \div 700$ K, function of concentration). The nanocrystals are thermally stable from 293K to T_c', due to the presence of Nb atoms which inhibit the crystallization process with heating [7], [9]. At higher temperatures ($T_c'' \sim 1000 \div 1200$ K), boride phase(s) appear (like Fe_2B, Fe_3B, etc.) and the alloys consist of different boride and intermetallic phases [5], [10], [13].

The hetero-coordinated distribution of Fe and Si atoms determines the features of total atomic distribution in the alloy.

Consequently, the Fe-Si-B-Nb-Cu alloys are multi-phases structures after crystallization and phases' structure and concentration evolve with temperature. For example, the $Fe_{73.5}Si_{13.5}B_9Nb_3Cu_1$ is a body-centred cubic (*bcc*) solid solution, composed of Fe_2Si + Fe_2B + $(Fe,Si)_3B$ + FeB [5]. The average lattice parameter is of 4.86 Å. The Fe_2B and FeSi solid solution are stable phases, present after crystallization.

Each alloy phases configuration was considered at simulations. Details of structure are presented in Fig. 1.

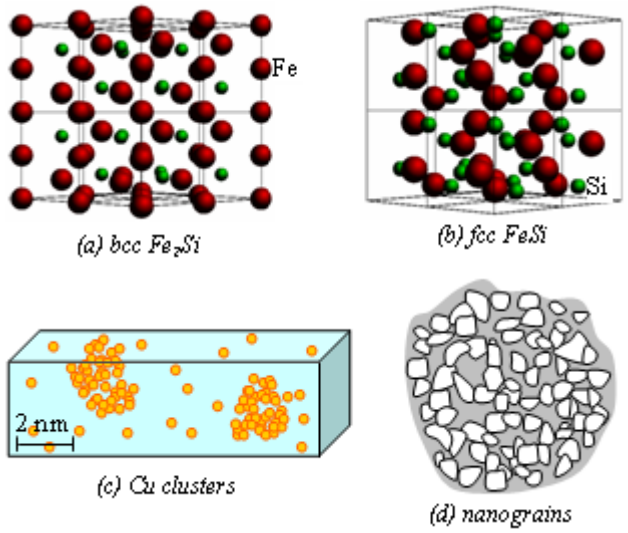

Fig. 1. Structure details for the Finemet alloys: (a) bcc lattice fragment; (b) fcc lattice fragment (lattice parameter of 4.62 ÷4.92 Å for the iron compounds); (c) agglomerations of Cu clusters in the solid solution space with multiple lattices; (d) nanograins (size of 5 - 20 nm) in the residual amorphous matrix.

The different alloy samples were simulated as 100 μm thick films, deposed onto a ceramic substrate of 1.8 mm thickness. Substrates are placed inside a rectangular waveguide with the cross-section of 22.86x10.16 mm, like in Fig. 2. Substrate length is of 18 ÷ 25 mm, in function of the operating frequency. The magnetic polarization field is $\boldsymbol{H_0}$ = 500 Oe. The simulational exposure configuration reproduces the experimental arrangement used for determination of the *S*-parameters for the material samples in microwave range, in our laboratory. Experimental installation can be exploited for broadband measurement of the permeability tensor components and of the complex permittivity of the SMC and of ferrimagnets.

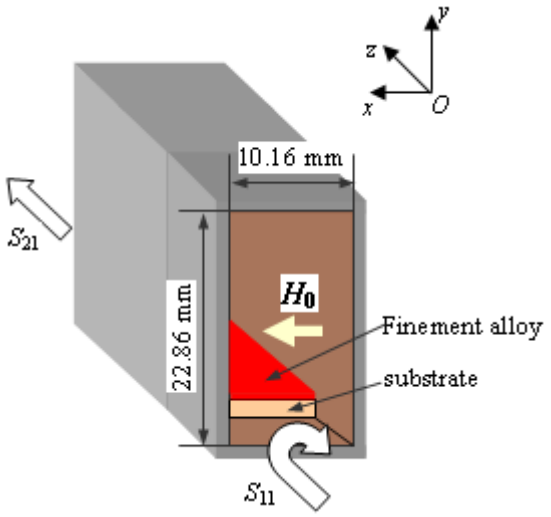

Fig. 2. Thick films (100 μm*) of Finemet alloys deposed on a ceramic substrate inside a rectangular waveguide. Simulational and experimental arrangement.*

The *S*-parameters (reflection and transmission coefficients) of the experimental device are directly related to electromagnetic properties of the considered material. The *S*-parameters are measured using a vector network analyzer: HP 8720 A (130 MHz - 20 GHz). At simulations, the HFSS program uses the finite elements method to determine the electromagnetic field distribution and to extract reflection and transmission coefficients of the TEM mode, determined by the presence of the magnetic material. Ports were de-embeded for obtaining the right values of the *S*-parameters at samples boundaries.

The sample electric permittivity and magnetic permeability were determined from these coefficients and from the electromagnetic analysis of the discontinuities created within the material [11]. Maxwell's equations were written, in order to consider the electrical conductivity of the medium trough an overall expression of permittivity.

By frequency sweeping, simulations and measurements were performed in microwave range (1-10 GHz), in order to obtain the permeability tensor components and the complex permittivity of the considered Finemet alloys. The relative values of these quantities were denoted as:

$$\underline{\underline{\mu}} = \begin{bmatrix} \mu & -j\kappa & 0 \\ j\kappa & \mu & 0 \\ 0 & 0 & 1 \end{bmatrix}, \tag{1}$$

with $\mu = \mu' - j\mu''$, $\kappa = \kappa' - j\kappa''$;

$$\varepsilon = \varepsilon' - j\varepsilon'', \tag{2}$$

respectively (j represents the imaginary unit: $j^2 = -1$). Real and imaginary parts were determined separately in each case, for physical interpretations.

3. Results for the material parameters

3.1. Magnetic permeability

The Fe-Si-B-Nb-Cu Finemet alloy characteristics are: high magnetic permeability and high electrical resistivity. The material analysis by simulation and measurements has to relieve these characteristics and to point out the particularities of the frequency evolution of the constitutive parameters. The multi-phases structures at the atomic scale present magnetic anisotropy, consequently the components of the permeability tensor have to be determined, for the considered frequency range (1 - 10 GHz). The results obtained by structural simulations and measurements are presented in Fig. 3, for the $Fe_{73.5}Si_{13.5}B_9Nb_3Cu_1$ alloy. Curves obtained for the other considered Finemet alloys present similar frequency evolution, but with different peak frequency and magnitude, respectively with slightly different increasing/decreasing slopes. The specific features for each alloy composition are the peak frequencies and the results accuracy, illustrated in Table 1.

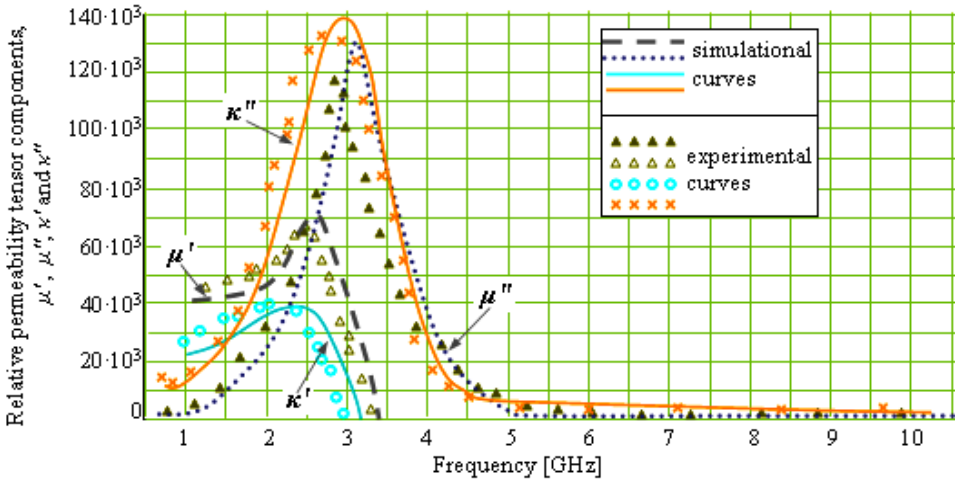

Fig. 3. Relative permeability tensor components, μ', μ", κ' and κ", for the $Fe_{73.5}Si_{13.5}B_9Nb_3Cu_1$ alloy. Results obtained by simulations and measurements were illustrated on graph.

Table 1. Peak frequencies corresponding to the frequency evolution of the relative permeability tensor components, μ', μ", κ' and κ", for the considered Fe-Si-B-Nb-Cu alloy. Results were obtained by simulations and measurements. The percentage relative errors of the simulational results in respect with the measurements were indicated in the table. Minimum errors were bold written.

No	Alloy	Peak frequency [GHz] (simulated/measured)				Relative error of the simulational results [%]			
		$max_{\mu'}$	$max_{\mu"}$	$max_{\kappa'}$	$max_{\kappa"}$	$er_{\mu'}$	$er_{\mu"}$	$er_{\kappa'}$	$er_{\kappa"}$
1.	$Fe_{74.5}Si_{13.5}B_9Nb_3$	1.663/ 1.537	2.216/ 1.998	1.943/ 1.653	2.287/ 2.046	8.20	10.91	17.54	11.78
2.	$Fe_{76.5}Si_{13.5}B_9Cu_1$	1.716/ 1.624	2.298/ 2.166	2.176/ 2.023	2.463/ 2.302	5.66	6.09	7.56	6.99
3.	$Fe_{73.1}Si_{15.5}B_{7.4}Nb_3Cu_1$	2.586/ 2.413	3.027/ 2.791	2.328/ 2.106	2.875/ 2.628	7.17	8.46	10.54	9.40
4.	$Fe_{73.5}Si_{13.5}B_9Nb_3Cu_1$	2.643/ 2.486	3.129/ 2.865	2.441/ 2.173	2.966/ 2.723	6.31	9.21	12.33	8.92
5.	$Fe_{74.5}Si_{13.5}B_8Nb_3Cu_1$	2.823/ 2.621	3.625/ 3.426	2.821/ 2.418	3.229/ 2.943	7.71	5.81	16.67	9.718
6.	$Fe_{77.5}Si_{13.5}Nb_3Cu_1$	2.946/ 2.723	3.894/ 3.542	2.963/ 2.676	3.452/ 3.184	8.189	9.938	10.725	8.417
7.	$Fe_{77.5}Si_{11.2}B_{7.2}Nb_{3.3}Cu_{0.8}$	2.423/ 2.217	3.026/ 2.813	2.314/ 2.095	2.843/ 2.585	9.292	7.572	10.453	9.981
8.	$Fe_{73.2}Si_{13.7}B_{9.5}Nb_{2.7}Cu_{0.9}$	2.894/ 2.753	3.337/ 3.245	2.748/ 2.584	3.166/ 2.989	**5.122**	**2.835**	**6.347**	**5.922**
9.	$Fe_{68.8}Si_{18.6}B_{9.5}Nb_{2.6}Cu_{0.5}$	2.757/ 2.606	3.279/ 3.127	2.618/ 2.404	3.012/ 2.813	5.794	4.861	8.902	7.074

Accuracy of the determinations was calculated by reporting the simulation results to the results of the measurements. One observes that the composition without Cu (alloy no. 1) has the lowest peak frequencies and the maximum errors for the simulation results. This is due to the increased percent of amorphous phase after crystallization, in respect with other alloys (the Cu nucleation centres are missing, their role being partially assumed by the Nb atoms). Lower errors were obtained for the alloy without Nb (alloy no. 2), which influence less the crystallization process, but more the thermal stability of the alloy.

We have again less precise results for the alloy no. 6 (without boron, this time). This is due to the fact that the missing Fe-B phases are very stable (are formed at high temperatures) even the B concentration in the alloy is not very high. Generally, a simulated structure with variable phase concentration generates less precise results.

For the alloys presenting both Cu and Nb elements, the percent of crystalline phase is high enough in expense of the amorphous phase after crystallization (alloys present more nucleation centres). This fact increases the magnetic anisotropy of the alloy. Peak frequencies are shifting to higher frequencies, their magnitude is higher and the accuracy of the simulations is better. Small differences are determined by the Fe-Si phases concentration in the alloy (one are more stable then the others). If the heat treatment is done at temperature higher than 1200 ^{0}C, the resulting boride phases confer the greatest stability to the alloy, a potentially high ordered structure and consequently, the highest accuracy of structure simulations (see alloy no. 8, 9). On the contrary, the absence of the boron in alloy determines medium to high errors, but with proximate values for all tensor components (alloy no. 6). This is an effect of the more poor stability of phases in the alloy.

The simulational relative error is systematically positive if we consider the measurements results as reference (it is an error due to the method). This error has the advantage that can be minimized by errors optimization. The accuracy of the measurements was estimated to less than 4 % relative error, in respect with the best obtained result.

3.2. Electric permittivity

Determinations were performed for another constitutive parameter of the considered Finement alloys: the electric permittivity. Materials were simulated like complex multi-component structures. The macro-components are the nanograins and the micro-components are the co-existing phases of the solid solution: crystalline single phases (crystalline lattices as FeSi, Fe_2B, fcc Cu, etc.), residual amorphous matrix and single atoms (Nb, B eventually).

The real and imaginary components of each material permittivity were determined by simulations. Measurements were performed using the experimental arrangement described above (Fig. 2), in the frequency range of (1 - 10 GHz). The obtained results are exemplified with help of the simulational and experimental permittivity curves for the same $Fe_{73.5}Si_{13.5}B_9Nb_3Cu_1$ alloy, given in Fig. 4.

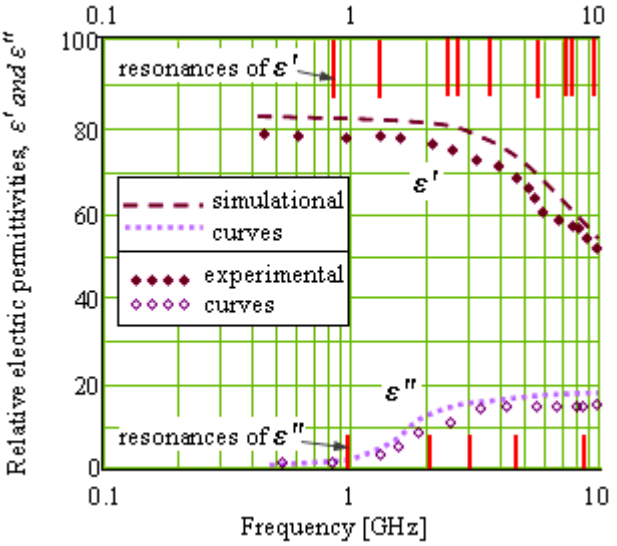

Fig. 4. Relative electric permittivities, ε' and ε'', for the $Fe_{73.5}Si_{13.5}B_9Nb_3Cu_1$ alloy, obtained by simulations and measurements. The permittivity resonance positions on frequency scale are indicated on graph.

One observes that the critical frequencies of the permittivity curves correspond to the permeability peaks indicated in Fig. 3. This is a consequence of the fact that the material responds similar to the electric and magnetic field, these fields being not independent (are included in the same physical entity: the electromagnetic field). These critical frequencies (or peak frequencies) correspond to the resonant phenomena when field interacts with the structure. In our case, for the Finemet alloys, simulations have indicated us that the geometrical characteristics of the Fe-Si phases impose the critical frequency values. By modifying the boron content in alloy, slight shifting of the critical frequencies was obtained. This is due to the high stability of the boride phases (of low concentration in fact), which were developing in expense of the Fe-Si phases, but at high temperatures (ca. 1200 K).

The same systematical error appears (the measured values are lower than the simulated ones), which can be eliminated by error optimization.

3.3. Electrical conductivity

An electrical resistivity value around 1.2 μΩ·m was reported for the Finemet alloys at low frequencies (hundred of kilohertz) [12], [14]. Materials are recommended as high electrical resistivity SMC (has resistivity as high as amorphous metallic alloys, like Pd-Cu-Si, the Metglas Fe-Ni-P-B, Zr-Ti-Cu-Ni-Be, bulk

amorphous steel, etc.). The LF resistivity value was taken as reference in this case, in order to start the iterative process at simulations.

Our results, obtained by simulation and measurements, illustrate the isothermal electrical resistivity evolution with frequency in the frequency range of 1 - 10 GHz. We have exemplified here with the electrical conductivity curves given in Fig. 5, for the same $Fe_{73.5}Si_{13.5}B_9Nb_3Cu_1$ alloy. The Finemet alloys present a conductivity increasing with frequency, more accentuate at lower frequencies (1-3 GHz) and then slower (over 3 GHz).

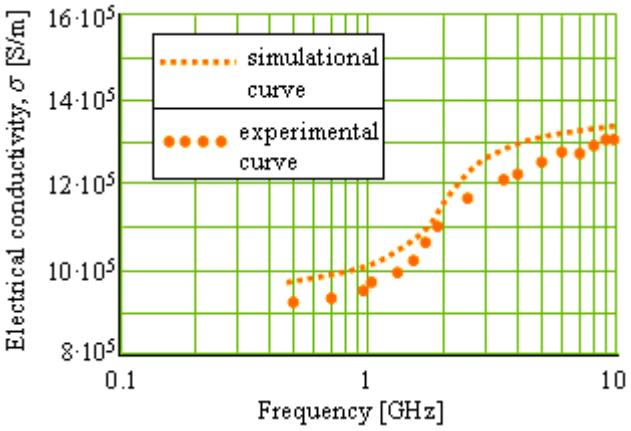

Fig. 5. Electrical conductivity for the $Fe_{73.5}Si_{13.5}B_9Nb_3Cu_1$ alloy, obtained by simulations and measurements.

One can observe similar position of the curve flexure point on frequency scale like in the case of the other constitutive parameters, position imposed by the Fe-Si phases. The low content of the B, Nb and Cu elements in the alloy can not modify significantly the conductivity. Low modification of the conductivity magnitude can be obtained for different characteristics of the heat treatment, by controlling the annealing time and speed. This affects directly the muti-phases structure of the alloy, obtained after crystallization. Simulations for the same alloy crystallized in different annealing condition have been performed and the results are available in our data base. Such of results indicate us contribution of each alloy phase at electrical resistivity.

4. Conclusions

The Finemet alloys with very good magnetic properties, lead-free materials and with high frequency use were considered in this paper. The Fe-Si-B-Nb-Cu alloys are multi-phases structures after crystallization and phases' structure and concentration evolve with temperature. Material analysis was performed for frequencies in microwave range (1 - 10 GHz), by structural simulation and measurements. Results were obtained for the constitutive parameters: magnetic permeability, electric permittivity and electrical conductivity, in case of Finement alloys with different concentrations of the constitutive elements. One points out the following conclusions by structural interpretation of the results:

- The composition without Cu has the lowest peak frequencies for the magnetic permeability tensor components and the maximum errors for the simulation results, due to the increased percent of amorphous phase after crystallization, in respect with other alloys (the Cu nucleation centres are missing). Lower errors were obtained for the alloy without Nb, which influence less the crystallization process, but more the thermal stability of the alloy.
- Less precise results were obtained for the alloy without boron, due to the fact that the missing Fe-B phases are very stable (are formed at high temperatures) even the B concentration in the alloy is not very high.
- For the alloys presenting both Cu and Nb elements, the percent of crystalline phase is high enough in expense of the amorphous phase after crystallization, fact that increases the magnetic anisotropy of the alloy. Peak frequencies are shifting to higher frequencies, their magnitude is higher and the accuracy of the simulations is better. Small differences are determined by the Fe-Si phases concentration in the alloy, phases which are more or less stable.
- If the heat treatment is done at temperature higher than 1200 K, the resulting boride phases confer the greatest stability to the alloy, a potentially high ordered structure and consequently, the highest accuracy of structure simulations. The absence of the boron in alloy determines more poor stability of phases in the alloy.
- The critical frequencies of the permittivity curves correspond to the permeability peaks. These critical frequencies (or peak frequencies) correspond to the resonant phenomena when the electromagnetic field interacts with the structure. Simulations have indicated us that the geometrical characteristics of the Fe-Si phases impose the critical frequency values. By modifying the boron content in alloy, slight shifting of the critical frequencies was obtained, due to the high stability of the boride phases, which were developing in expense of the Fe-Si phases, but at high temperatures (ca. 1200 K).
- On the conductivity versus frequency curves we have similar position of the curve flexure point on frequency scale like in the case of the other constitutive parameters, position imposed by the Fe-Si phases. Low modification of the conductivity magnitude can be obtained by controlling the annealing time and speed. This affects directly the muti-phases structure of the alloy, obtained after crystallization.

Our study was performed for the high frequency range and indicates us that the material properties obtained for this frequency domain are favorable for applications in the high technologies field. Effects of material good properties are: energy saving, high frequency use, size/weight reduction, noise suppression, magnetic and electro circuit designing. Consequently, Finemet alloys can be used for: magnetic amplifier, pulse power cores, surge absorbers, high voltage pulse transformers, saturable cores, EMI filters, common mode chokes, magnetic

shielding sheets, electromagnetic wave absorbers, current sensors, magnetic sensors, high frequency power transformers, active filters, smoothing choke coils, accelerator cavity.

Acknowledgements

The authors are grateful to Professor Emmanuelle Bourdel from Equipe micro-ondes of École Nationale Supérieure de l'Électronique et de ses applications, Cergy-Pontoise, France, for the technical advising.

References

[1] G. Herzer, Handbook of magnetic materials, ed. K. H. J. Buschow (Amsterdam: Elsevier Sci.), 320, (1997).
[2] B. Majumdar, D. Akhtar, Bull. Mater. Sci. **28**(5), 395 (2005).
[3] R. E. Coelho, R. M. Gomes, S. Jackson G. de Lima, Mat. Res.**8**(2)**,** 161, (2005).
[4] S. Matsumura, S. Takeuchi, Y. Tahara and K. Oki**,** J. of Electron Microscopy **42**(5), 310, (1993).
[5] P. Krakhmalev, D. Yi, L. Nyborg, Proc. 22nd Risø Inter. Symp. on Mat. Sci., Roskilde, Denmark, (2001).
[6] K. Hono, D. H. Ping, Proc. Inter. Conf. Solid-Solid Phase Transformations '99, May 24 - 28, Kyoto, Japan, (1999).
[7] S. Mudry, Yu. Kulyk, A. Korolyshyn and Yu. Plevachuk, Rev. Adv. Mater. Sci. **14,** 41, (2007).
[8] R. Jain, N. S. Saxena, K. V. R. Rao, D. K. Avasthi, K. Asokan, S. K. Sharma, Mat. Sci. and Eng. A 297, 105, (2001).
[9] X D. Liu, J. T. Wang, K. Lu, J. Zhu, J. Jiang, J. Phys. D: Appl. Phys. 27, 165, 1994.
[10] M. Godec, Dj. Mandrino, B. Šuštaršič, M. Jenko, Surface and Interface Analysis 34, 346, (2002).
[11] P. Quéffélec, M. Le Floc'h, P. Gelin, IEEE Trans. on Microwave Theory and Techniques **48**(8), 1344, (2000).
[12] W. Lu, L. Yang, B. Yan, H. Wen-Hai, Mat. Sci. & Eng. B **128(1-3)**, 179, 2006.
[13] S. Linderoth, Proc. 22nd Risø Inter. Symp. on Mat. Sci., Roskilde, Denmark, (2001).
[14] Finemet, Square Loop Cores, Technical Bulletin of Metglas, on-line: www.metglas.com.

*Corresponding author: danait@etc.tuiasi.ro